


Article

An Experimental Investigation of the Effects of Dressing and Grinding Parameters on Sustainable Grinding of Inconel 738 Used for Automated Manufacturing

Mohammadjafar Hadad ^{1,2}, Samareh Attarsharghi ^{3,*} , Javad Makarian ² and Ali Mahdianikhotbesara ²

¹ Department of Mechanical Engineering, College of Engineering and Technology, University of Doha for Science and Technology, Doha P.O. Box 24449, Qatar; mohammadjafar.hadad@udst.edu.qa or mjhadad@ut.ac.ir

² School of Mechanical Engineering, College of Engineering, University of Tehran, Tehran P.O. Box 11155-4563, Iran

³ Department of Electrical Engineering, College of Engineering and Technology, University of Doha for Science and Technology, Doha P.O. Box 24449, Qatar

* Correspondence: samareh.attarsharghi@udst.edu.qa

Abstract: The significant effect of the dressing process on the surface of the grinding wheel (GW) and the need to provide an optimal dressing condition are the requirements of reduction machining time and energy consumption in the sustainable grinding process. In this study, for the first time, the results of changes in the parameters of the dressing process and changes in the topography of the grinding surface on the surface roughness of the Inconel 738 have been presented using single-edge and four-edge diamond dressers. The use of minimum quantity lubrication (MQL) and wet condition are other variables in this study to reduce the consumption of cutting fluid and prevent its destructive effects on the environment. The results indicate that the MQL technique increases the grinding performance of Inconel 738 by reducing ground workpiece surface roughness and decreasing the coolant–lubricant consumption comparing to the conventional wet grinding process. Additionally, it has been found from the experimental results that applying a single-edge dresser generates finer topography on the grinding wheel and, consequently, has a better surface finish in the grinding process compared to the multipoint diamond dressing tool with the same dressing and grinding parameters. In other words, increasing the dressing feed rate during dressing of the grinding wheel using a multipoint dresser makes a finer wheel surface topography and as a result decreases the surface roughness of the ground workpiece compared to a single-edge dresser. With multipoint diamond tools, the grinding performance during the life of the dressing tool also tends to remain more consistent, which is a definite advantage in automated production. Therefore, application of a multipoint dresser leads to a reduction in dressing time and increased production capability.

Keywords: dressing; grinding wheel surface topography; minimum quantity lubrication (MQL); Inconel 738; surface roughness; chip loading



Citation: Hadad, M.; Attarsharghi, S.; Makarian, J.; Mahdianikhotbesara, A. An Experimental Investigation of the Effects of Dressing and Grinding Parameters on Sustainable Grinding of Inconel 738 Used for Automated Manufacturing. *Processes* **2023**, *11*, 2876. <https://doi.org/10.3390/pr11102876>

Academic Editors: Zhigang Jiang, Yan Wang, Yue Wang, Wei Cai and Jiaqiang E

Received: 3 September 2023

Revised: 26 September 2023

Accepted: 27 September 2023

Published: 29 September 2023



Copyright: © 2023 by the authors. Licensee MDPI, Basel, Switzerland. This article is an open access article distributed under the terms and conditions of the Creative Commons Attribution (CC BY) license (<https://creativecommons.org/licenses/by/4.0/>).

1. Introduction

Nickel-based superalloys are creep-resistant materials that work at high temperatures. These materials are used to manufacture hot parts for aircraft and rocket engines, gas and steam turbines, heat exchangers, and boilers. In these alloys, refractory and carbide-forming elements with high melting points, such as tantalum, molybdenum, chromium, cobalt, and tungsten, and sedimentary phase elements, such as titanium aluminum, have been used. Superalloys are heat-resistant alloys based on nickel, iron, and cobalt that often operate at temperatures above 500 °C. By combining properties such as strength, creep resistance, fatigue strength, and corrosion resistance, they can work at high temperatures for long periods. The combination of high temperature resistance and resistance to oxidation and

corrosion of these materials is unmatched by other metallic materials. For these reasons, superalloys are often used in hot parts of jet turbine engines, such as blades and combustion chambers, rocket engines, power plant turbines, heat treatment equipment, and chemical and petrochemical units. The metallurgical properties and microstructure, and chemical composition of these alloys affect their creep behavior [1,2]. The grinding of this material is always tricky due to its high strength and thermal resistance. Surface burns, GW wear, GW surface loading, and high-cutting fluid consumption are some of the grinding problems of this material [3–8].

Optimization of grinding surface topography is one of the most important challenges in industries in order to reduce chip loading on the grinding wheel surface and at the same time decrease the utilization of grinding coolant lubricant [8–12]. The topography of the GW and the geometry of the grain cutting edges are basic to cutting the parts. The topography of the GW surface, the geometry of the cutting edges, and variables such as the sort of bond and grain size are the work of planning the GW surface before grinding. After grinding, the scraped area of the grains and chips are stuck to the surface of the GW; in other words, stacking the GW, applying single-edge, multi-edge, sharpening and truing tools to move forward the grinding operation are unavoidable. When the tool hits the surface of the GW, the breakage of grains and chips connected to the GW surface leads to changes in topography and diminishes the stack on the GW. The feed rate of the dresser in the axial direction for each dressing pass of the GW is called the dressing pitch and is obtained from Equation (1) as follows [13]:

$$\left(S_d = \frac{\pi d_s V_{fd}}{V_s} \right) \quad (1)$$

So that V_{fd} is the feed rate of the dresser, V_s is the grinding wheel speed, and d_s is the diameter of the GW. Therefore, the dressing tool follows a path that would appear to be cutting a thread on the abrasive grains with a pitch (lead), S_d . If the single-edge tool has a radius r_d , the theoretical roughness created on the surface of the GW is obtained by Equation (2) as [13]:

$$\left(R_{ts} = \frac{S_d^2}{8r_d} \right) \quad (2)$$

Equation (2) demonstrates how different factors affect the quality of a grinding wheel's surface in a grinding process. A larger dressing lead (S_d) and a sharper dressing tool (smaller r_d) tend to make the wheel surface rougher, while the dressing depth (a_d) does not have an impact. The influence of the dressing lead on the grinding wheel's surface has been confirmed through profiles of ground workpieces in [13]. In other words, the quality of grinding processes is significantly influenced by the preparation of the grinding wheel. This preparation involves achieving the required grinding wheel profile and creating the appropriate wheel topography, which affects the surface quality of the workpiece. The specific distribution of abrasive grains on the grinding wheel's surface plays a crucial role in shaping its topography.

The topography of the grinding wheel plays a paramount role as an input parameter in the grinding process [14–17]. This topography can be affected by wear during grinding. Additionally, the dressing process involves active mechanisms such as grit breakage, bonding breakage, grit break-out from the bonding, or grit deformation [18–22]. Table 1 provides a concise summary of the research background related to the dressing process. Despite its significant impact on grinding performance, the setup of the dressing process is frequently carried out through empirical or theoretical approaches, utilizing both single-point diamond stationary dresser tools and rotary diamond dressers in dry and wet grinding processes.

Table 1. Grinding wheel dressing research background.

Investigator	Year	Research Condition	Results
Pande et al. [14]	1979	Effects of dressing parameters on GW performance	Achieve optimal mode for dressing feed and depth
Li et al. [15]	2006	Wear of diamond GWs in grinding of silicon nitrides	The importance of sharpening in diamonds as well as providing the optimal mode of dressing depth for silicon nitride
Linke et al. [16]	2010	Temperature and wear mechanism in dressing of vitrified bonded GWs	Diamond dressers' wear mechanism and factors and their effect on ground surface roughness
Daneshi et al. [17]	2014	Effects of dressing parameters on internal grinding	Investigation of the effect of GW diameter and dressing method on roughness and geometrical form and quality of holes in the grinding process
Klocke et al. [18]	2008	Mechanisms in the generation of GW topography by dressing	Investigating of the effect of dressing and GW structure on the formation of workpiece surface defects and roughness
Deng et al. [19]	2019	A review on dressing strategies of super abrasive GWs	Offering a variety of different methods of GW dressing
Hadad et al. [20]	2016	Investigation of the effects of dressing and wheel topography on grinding process using different coolant–lubricant conditions	Effect of single point diamond dressing parameters on the roughness of the workpiece and reduction in cutting fluid consumption
Moreno et al. [21]	2020	Friction improvement by GW texturing using dressing process	Produce different GW surface topography in a controlled dressing process to reduce friction coefficient
Zhou et al. [22]	2019	Dressing technology of arc diamond wheel by roll abrading in aspheric parallel grinding	Improve dressing and grinding performance of arc diamond wheels

Traditional coolant lubricants (petroleum-based fluids) contain chlorine, phosphorus, and sulfur compounds. These compounds are harmful to the environment and humans. These cutting fluids lead to operators' skin, respiratory, and sometimes gastrointestinal diseases. Another issue is the nondegradability of these fluids in the environment. Using a cutting fluid nozzle that can adjust the flow rate and deliver cutting fluid effectively into the cutting zone is one of the traditional methods of cooling and lubricating. The traditional method of delivery of the coolant lubricant to the machining zone is also called wet (fluid) machining. Environmental issues and problems have increased the desire of industrialists and production researchers to eliminate cutting fluid from manufacturing processes. For a long time, much advantage has been derived from machining without utilizing cutting liquids or using a minimum amount of coolant lubricant. When no cutting fluid is used as a coolant lubricant in the machining process, it is called dry machining. When the minimum amount of cutting fluid is utilized in the cutting zone, it is called semidry machining or minimum quantity lubrication (MQL) machining. Dry machining is the best arrangement environmentally. Dry machining has benefits such as no air pollution, no problems with cutting fluid disposal, and reduced risk to operator health. However, in dry machining, conditions must be met to compensate for the initial tasks of the cutting fluid, including lubrication, cooling, and chip removal from the cutting zone. In MQL machining a minimal amount of lubricant is sprayed into the machining zone. This method has been developed as an alternative to dry and conventional wet machining techniques. In MQL machining, the cooling medium is a mixture of air and oil sprayed so that the suspended oil droplets are dispersed in the air jet and sprayed periodically to the cutting zone. Small droplets of oil are transported directly by air to the tool-workpiece contact zone, and both cooling

and lubricating are performed. Table 2 shows the research background in applying the MQL technique during grinding processes. The literature review shows the lack of study on the effects of stationary dresser types as well as the grinding wheel surface topography on grinding performance in minimum quantity lubrication-MQL grinding of Inconel 738.

Table 2. MQL research background.

Investigator	Year	Research Condition	Results
Hoffmeister et al. [23]	1998	100Cr6 (60HRC) and application of liquid nitrogen with MQL with ester oil and corundum GW with vitrified bond	Reduction of forces, reduction in roughness, reduction in GW wear
Baheti et al. [24]	1998	AISI 52100 (60HRC) using ester oil and corundum GW with vitrified bond	Reduce specific power and energy, reduce GW wear, increase roughness
Tönshoff et al. [25]	1994	16MnCr5 (58HRC) and application of ester oil and corundum GW with vitrified bond and comparison with conventional wet grinding with mineral oil	Reduction of grinding forces, an increase in roughness
Brockhoff et al. [26]	1998	16MnCr5 (58HRC) and application of ester oil and corundum GW with vitrified bond	Increased roughness and grinding forces, applicability in $Q_w < 5 \text{ mm}^3/\text{mm}\cdot\text{s}$
Klock et al. [27]	1997	16MnCr5 (58HRC) and application of ester oil and corundum GW with vitrified bond	Reduction of grinding forces, an increase in roughness, and type of coolant/lubricant has effects on performance.
Hafenbraedl et al. [28]	2000	AISI 52100 (60HRC) and application of ester oil and internal cylindrical grinding and corundum GW with vitrified bond	Reduce specific power and energy, reduce GW wear, increase roughness
Silva et al. [29]	2005	ABNT4340 (60HRC) and application of vegetable oil and corundum GW with vitrified bond and CBN GW	Reduction of tensile residual stress on the surface, reduction in force and roughness
Tawakoli et al. [21]	2010	100Cr6 and SG corundum GWs with vitrified and resin bond	Reduction of roughness, grinding forces, increase in efficiency, effective lubrication by choosing the right type of coolant–lubricant GW
Shen et al. [29]	2008	Dura-Bar 100-70-02 ductile iron (50HRC) and corundum GW with vitrified bond and CBN GW with vitrified bond and application of Nano-fluids in grinding	Reduction of forces and roughness and GW wear, increase in lubrication property
Lee et al. [30]	2010	SK-41C (Tool Steel), CBN GW, use of MQL with Nano-fluids (diamond and paraffin nanoparticles)	Reduction of grinding force and roughness of the workpiece compared to MQL and dry, positive effect of nanofluid used on surface quality
Hadad et al. [31]	2012	Hardened (100Cr6) 2 ± 50 Rockwell C, Al_2O_3 GW grinders (89A60I6V217, 89A36I8V217), and application of Hacoform20–34 oil	Reduce force and roughness by increasing the oil flow rate and air pressure and the optimal nozzle distance to the grinding area
Mao et al. [32]	2014	Use vegetable oils (soy, palm, and canola), liquid paraffin	Nanofluid with palm oil and molybdenum disulfide particles has the best lubrication properties, the best choice for proper heat transfer and lubrication performance
Rabiei et al. [33]	2014	Use of mild steels (CK45, S305) and hard steels (HSS, 100Cr6), Al_2O_3 GW grinders, MQL, Dry, Wet conditions,	MQL in both types of steel causes a reduction in grinding force and coefficient of friction, better surface quality in hard steels and poor surface quality in soft steels
Setti et al. [34]	2015	Ti-6Al-4V, GC60K5V GW, use of nanofluids (water with Al_2O_3 nanoparticles and water with CuO nanoparticles) with different concentrations for MQL	Reduction of friction, tangential force, grinding zone temperature, formation of c-shaped chips
Hadad et al. [35]	2020	A novel approach to improve environmentally friendly machining processes using ultrasonic nozzle–minimum quantity lubrication system	Improve droplet size and distribution and spray performance, improve surface quality

Henceforth, to delve into the enhancement of MQL performance in the grinding of Inconel 738, this study pioneers the exploration of the impacts of dressing parameters and grinding wheel topography. In essence, the investigation involves altering dressing methods, dressing depth, and dressing speed while preparing vitrified Al_2O_3 grinding wheels with two distinct stationary dressing tools: single-point and four-point diamond

dressers. Subsequent to the dressing of these grinding wheels, machining tests were carried out to assess the effects of wheel topography and the types of coolant lubricants on grinding performance. Performance parameters under scrutiny encompassed workpiece surface quality and wheel loading. These tests were conducted under both fluid-based and MQL conditions.

2. Materials and Methods

In order to perform the grinding process, a Prompt 300–1000 grinding machine-TAICHUNG City-Taiwan was used. Also, a precise table with a screw and nut mechanism was used to provide a variety of dressing feed rates during preparing and dressing process. The experimental set up and values were chosen based on the preliminary tests and the data collected from turbine blade manufacturer. Figure 1 shows the schematic of the experimental setup.

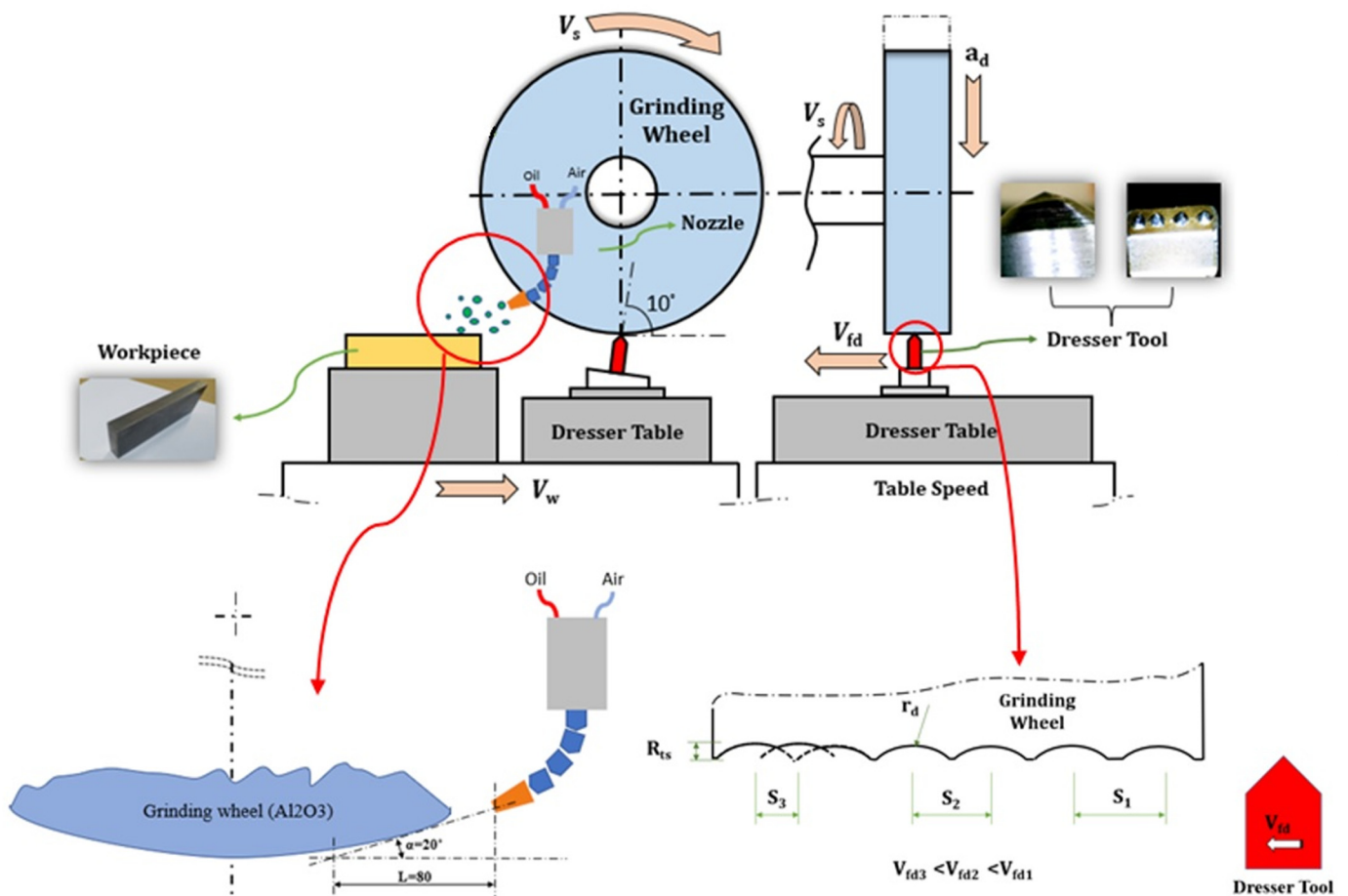


Figure 1. Schematic of the dressing and grinding process.

The system used to regulate the MQL was a custom-made setup that generated an air envelope, functioning as the mixing chamber, through the Venturi effect. Figure 2 shows the MQL nozzle and experimental set up for this study. One of the most important factors that should be considered in the grinding process with minimum lubrication is the position of the MQL nozzle relative to the grinding area. According to primary experiments, the MQL spray distance to contact zone (d) and the horizontal angle of the MQL nozzle to the workpiece (α) have been set as 80 mm and 20° , respectively. A summary of the experimental configuration and grinding parameters can be found in Table 3. Prior to each experiment, the grinding wheel underwent three dressing cycles with varying dressing conditions, which are also detailed in Table 3. The material properties of Inconel 718,

employed in this investigation, are provided in Table 4. The workpiece's surface roughness was quantified using a Mahr Surf PS1 Model-Germany, a portable roughness measurement device, employing a cut-off length of 0.8 mm in accordance with DIN EN ISO 3274:1998 standards [36]. After each test, Rz values were obtained at five distinct locations along the grinding direction to characterize the ground surface. Surface morphology and chip loading were examined using a digital microscope (DigiMicro, manufactured by DNT Company, Redditch, UK) capable of magnifying up to 200 times. Furthermore, images of chips and grains isolated from the grinding surface were scrutinized through an optical microscope from Optimums-Germany.

Table 3. Grinding conditions.

Type of Grinding Process	Flat Grinding
Grinding wheel	Al ₂ O ₃ (WA60K9V), Vitrified band, outer diameter: 450 mm
Surface grinding machine	Surface grinding machine MST-300-1000
GW rotational speed	2000 RPM
GW speed (v_c)	$v_c = 47$ m/s
Table feed rate (v_{ft})	$v_{ft} = 4.5\text{--}15$ m/min
Grinding depth of cut (a_e)	$a_e = 30$ μ m
Grinding environment	Cutting fluid, MQL (air-oil mixture)
Fluid used in grinding with cutting fluid and dressing operation	Water-soluble oil with a concentration of 5%
Cutting fluid flow rate in wet grinding	4 L/min
Oil flow rate in MQL grinding	200 mL/h
Air pressure in MQL grinding	5 bar
MQL oil	Vegetable oil
MQL oil viscosity (at 20 °C)	84 cP
MQL nozzle horizontal distance to GW	80 mm
Workpiece	Inconel 738 (16 × 40 × 200 mm)
Dressing tool	Single-edge, four-edge diamond tools
Dressing depth (a_d)	$a_d = 2, 5, 10, 20$ μ m
Dressing feed rate (v_d)	$v_d = 50, 85, 213, 420, 600$ mm/min
Dresser attack angle (α_d)	$\alpha_d = 10^\circ$
Number of dressing passes	$N_{dt} = 3$

Table 4. Material properties of Inconel 718 [8].

Density (kg/m ³)	Young's Modulus (GPa)	Poisson's Ratio	Thermal Conductivity (W/(m K))	Thermal Expansion Coefficient (K ⁻¹)	Specific Heat (J/(kg K))	Shear Modulus (GPa)
8220	208	0.3	11.4	1.3×10^{-5}	203	67.8

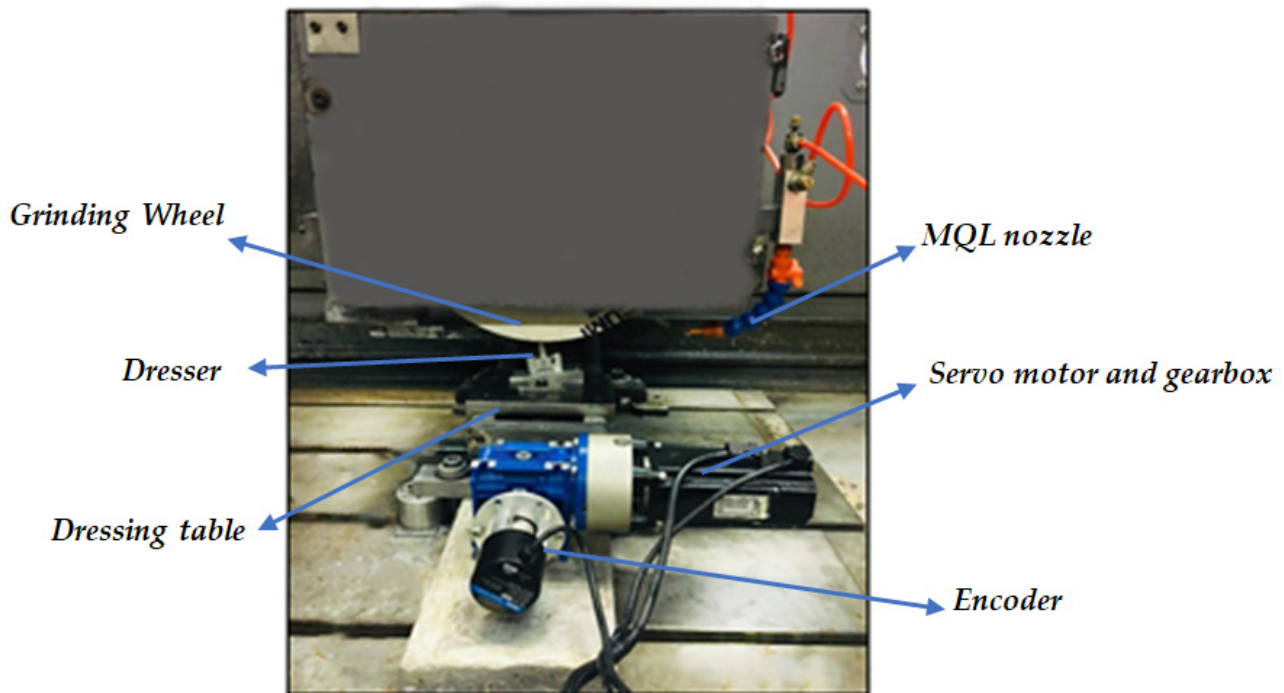


Figure 2. Experimental set up.

3. Results and Discussion

3.1. Grinding of Inconel 738 Using Single-Edge Diamond Dresser

Figure 3 shows the size distribution of particles removed by a single-edge diamond dresser under different conditions. Also included for comparison is the average particle-size distribution of the original 60 grit monocrystalline aluminum oxide used in manufacturing these wheels. It can be found from this figure that the coarser grains are collected at a depth of dressing of 10 μm . Larger grain sizes indicate the formation of a rough structure on the surface of the GW. Figure 4 shows wheel topography after different dressing conditions. As depicted in this figure, it is evident that an increase in dressing depth and feed rate leads to the creation of a rough surface topography on the GW, resulting in higher surface roughness on the machined workpiece surface. While bond fracture primarily governs the number of potentially active grains remaining on the wheel surface, the actual shape and condition of these grains are predominantly influenced by grain fracture, which operates on a much finer scale, and even by plastic deformation [20].

Workpiece surface roughness values (Figures 5 and 6) indicate that the MQL technique in grinding of Inconel 738 has significant effects on the grinding performance, while reducing the consumption of the cutting fluid from 4 L per minute to 200 mL per hour. In addition, increasing lubrication and increase in elastic-plastic deformation under the cutting edge of the abrasive grain results in decreasing the chip thickness and consequently lead to a reduction in surface roughness. On the other hand, by increasing the dressing feed and generating a coarse topography on the grinding wheel surface, the ground workpiece surface roughness increased. One of the factors increasing the workpiece surface roughness is the penetration of more grains into the workpiece. Increasing the table speed during grinding will result in penetration of more grains, which is shown in Figures 5 and 6 for different machining conditions.

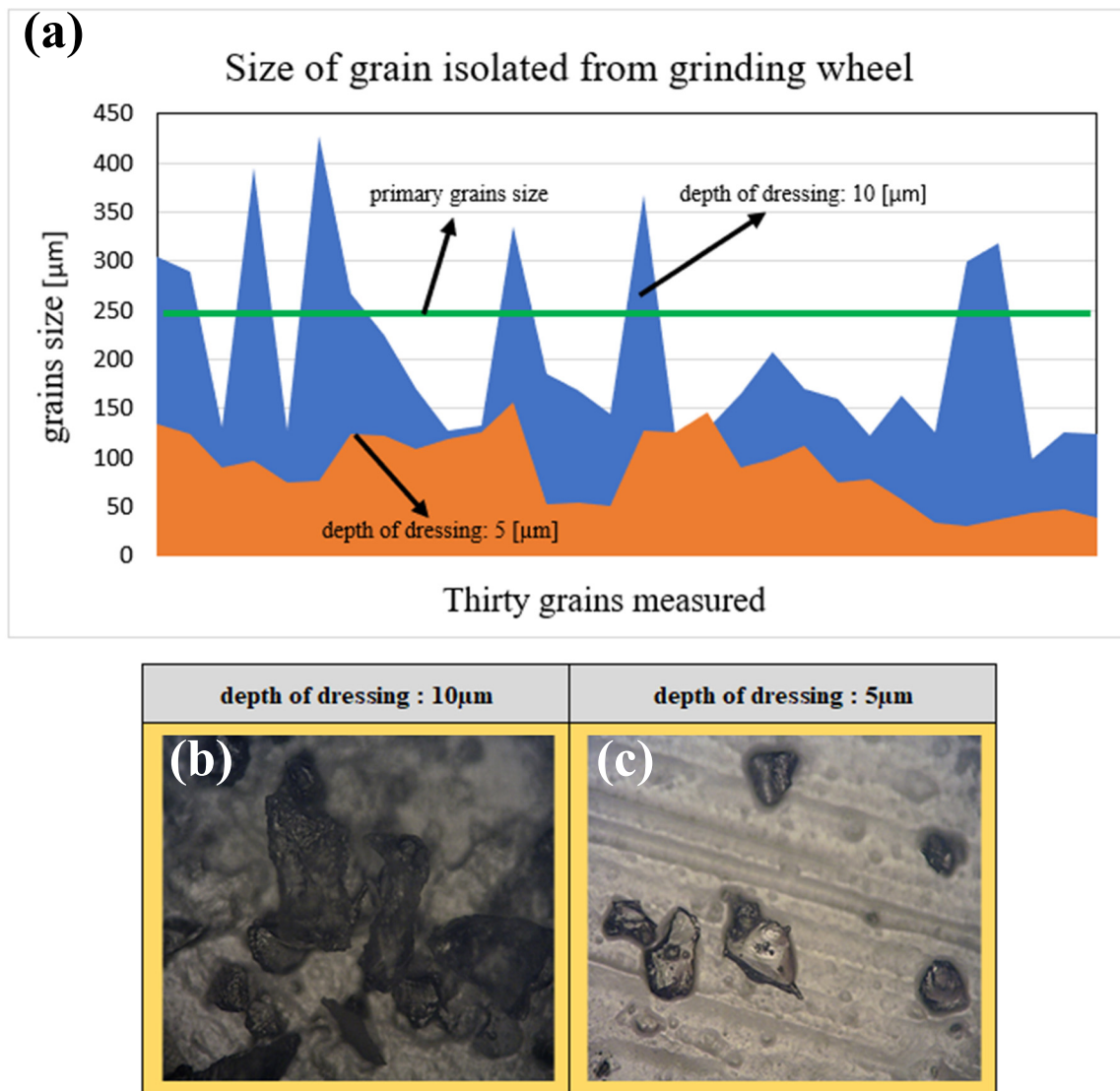


Figure 3. (a) grain size distribution of particles removed by single-point dressing measured using Image J 1.52v software, (b) grains obtained after dressing depth of 10 μm , (c) grains obtained after dressing depth of 5 μm ; (the average diameter of the original grain is included for comparison); $V_d = 420 \text{ mm/min}$ (magnification $\times 500$).

Surface morphology of ground workpieces and abrasive grain loading and chip morphology under different dressing and grinding conditions by applying a single-edge dresser are shown in Figures 7 and 8. Wheel surfaces with less loading of GWs in the conventional fluid grinding are essential and effectively reduce the number of required dressing processes in wet grinding operations. Due to the higher convection heat transfer coefficient of conventional applications of cutting fluids in wet grinding, the grinding zone temperature is much lower than that in MQL grinding, which results in melting of the chips and adhering to the GW surface in the MQL technique. As a result, the chip loading density on the GW surface is lower in wet grinding compared with MQL grinding. Due to the higher fluid flow rate in wet grinding and, consequently, better chip removal from the grain surfaces and the porosity of the GW, the GW loading is also lower in wet grinding than chip loading in the MQL technique.

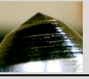
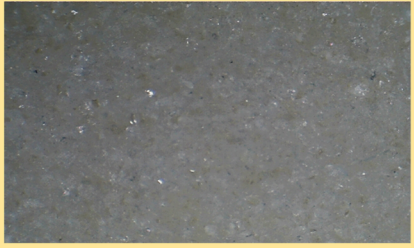



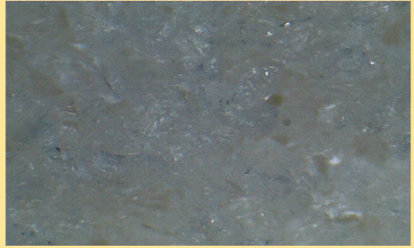


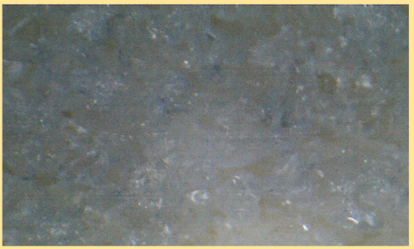
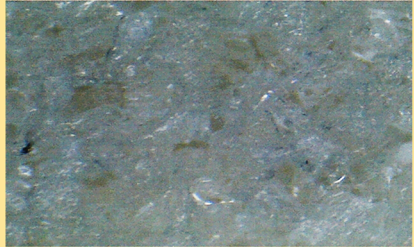
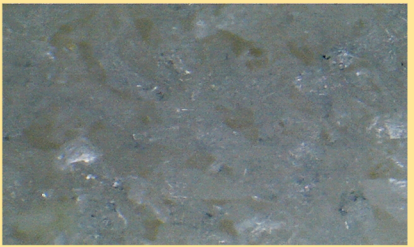
Single edge dresser		
Depth of dressing = 10 μ m	Depth of dressing = 5 μ m	
		$V_d = 50$ [mm/min]
		$V_d = 85$ [mm/min]
		$V_d = 213$ [mm/min]
		$V_d = 420$ [mm/min]
		$V_d = 600$ [mm/min]

Figure 4. Wheel surface topography after different dressing conditions using single-edge diamond dresser (magnification: 200 \times).

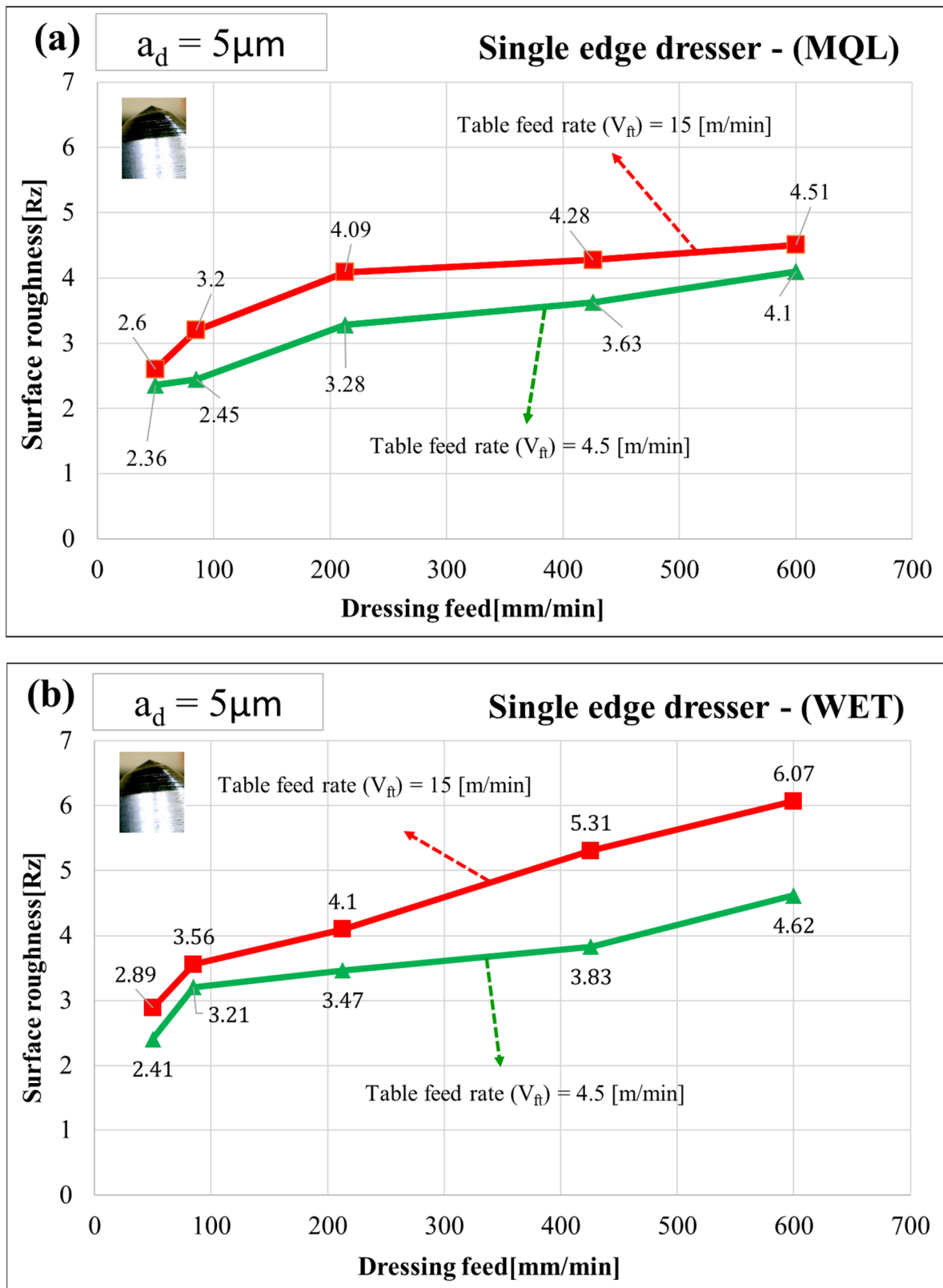


Figure 5. Workpiece surface roughness vs. dressing speed for dressing depth of 5 μm and single-edge dresser after (a) MQL grinding, (b) wet grinding.

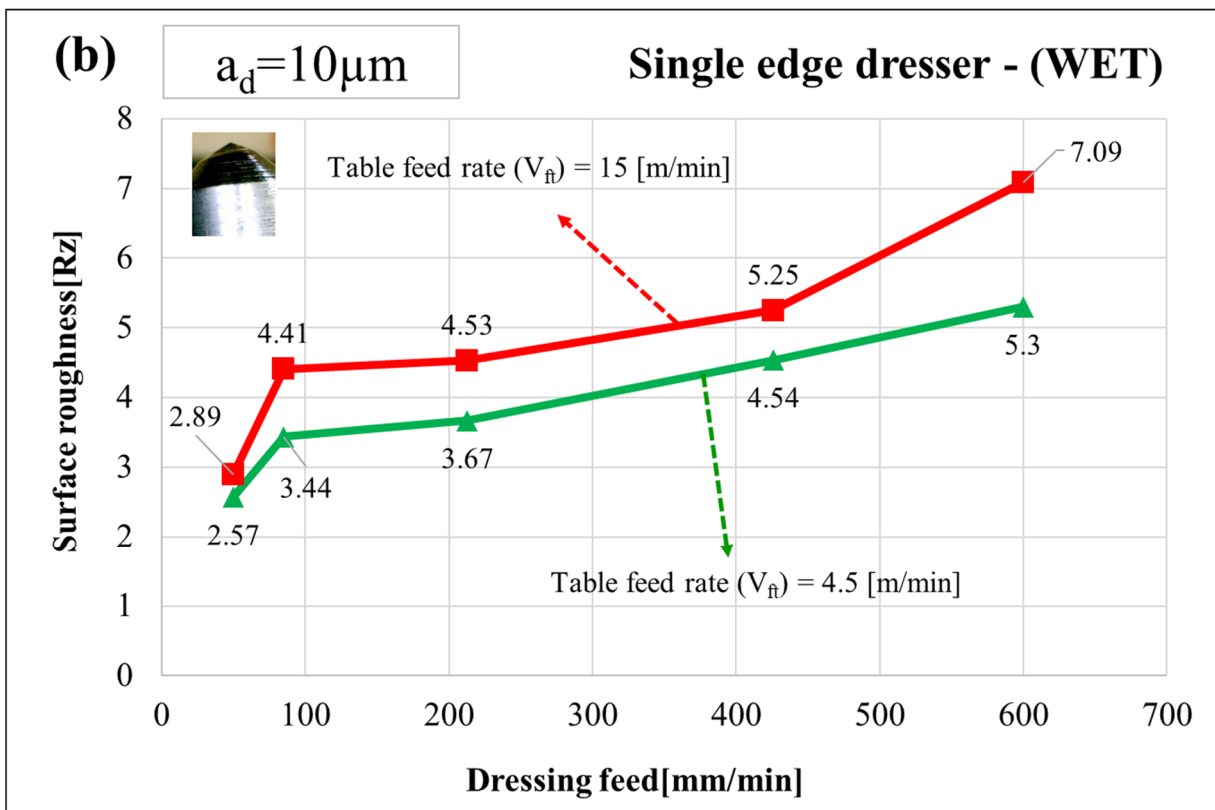
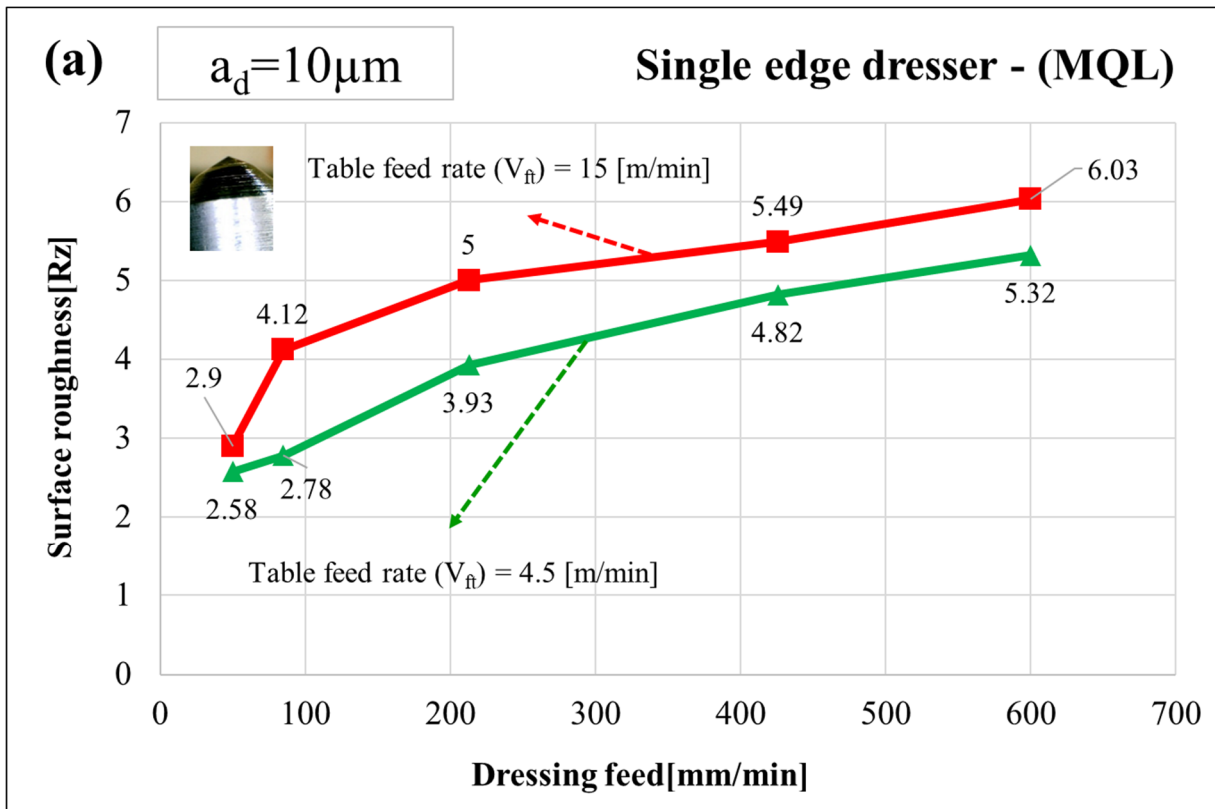


Figure 6. Workpiece surface roughness vs. dressing speed for dressing depth of 10 μm and single-edge dresser after (a) MQL grinding, (b) wet grinding.

MQL condition -(a)- Single edge dresser					Parameters		
grinding wheel	workpiece	[m/min]	grinding wheel	workpiece	[mm/min]	[μm]	[m/min]
		$a_d=10$			$V_d=50$	$a_d=5$	
			$V_d=213$				
			$V_d=600$				

Wet condition -(b)- Single edge dresser					Parameters		
grinding wheel	workpiece	[μm]	grinding wheel	workpiece	[mm/min]	[μm]	[m/min]
		$a_d=10$			$V_d=50$	$a_d=5$	
			$V_d=213$				
			$V_d=600$				

Figure 7. Surface morphology of ground workpieces and chip loading using single-edge dresser and (a) MQL grinding, (b) wet grinding ($a_e = 30 \mu\text{m}$, $V_c = 47 \text{ m/s}$) (magnification: $200\times$).

MQL condition- Single edge dresser			Wet condition- Single edge dresser				Unit
Chip	grinding wheel	(a)	Chip	grinding wheel	(b)		
		$V_d=50$			$V_d=50$	$a_d=10[\mu\text{m}]$	[mm/min]
		$V_d=213$			$V_d=213$		
		$V_d=600$			$V_d=600$		

Figure 8. Chip loading and chip morphology using single-edge dresser and (a) MQL grinding, (b) wet grinding ($a_e = 30 \mu\text{m}$, $V_c = 47 \text{ m/s}$, $V_{ft} = 4.5 \text{ mm/min}$) (magnification: $200\times$).

3.2. Grinding of Inconel 738 Using Four-Edge Diamond Dresser

Figures 9 and 10 compare the average surface roughness across the grinding direction for different wheel topographies and coolant–lubricant types when a four-edge diamond dresser has been used to prepare GW. As indicated by Equations (1) and (2), an increased dressing feed rate is associated with a coarser surface on the grinding wheel, while the dressing depth is seemingly unaffected. Furthermore, coarser dressing of the wheel typically leads to lower grinding forces and rougher workpiece finishes, whereas finer dressing results in higher forces and smoother workpiece surfaces. Figures 5, 6, 9 and 10 illustrate that among the two dressing methods and various dressing and grinding parameters, the dressing feed rate exerts a considerably greater relative impact on grinding performance when compared to the dressing depth. However, Figures 9 and 10 show that by decreasing the dressing feed rate lower than values of 213 mm/min (in soft dressing conditions), the ground surface roughness increases significantly. Accordingly, additional experiments were performed at depths of dressing of 2 and 20 μm as reported in Figures 11 and 12 for single and four edge dressers, to examine and verify the results of Figures 5, 6, 9 and 10 for lower and higher dressing depths. Although bond fracture primarily governs the number of potentially active grains remaining on the wheel surface, the shape and condition of these grains are predominantly influenced by grain fractures on a much smaller scale and, in some cases, even by plastic deformation. Despite the inherent brittleness of conventional ceramic grain materials, they can still undergo plastic deformation during dressing, as evident from the micrograph images of the GW surface. To compare the effect of single-edge and four-edge dressers on the morphology of the wheel surface, the images of the wheel surface after dressing are shown in Figure 13. In this particular scenario, both the dressing lead and dressing depth were relatively modest. When using a single-edge dresser, there is minimal deformation, and the grains exhibit a higher degree of fragmentation. In a broader context, both grain fracture and plastic deformation are significant factors. Conversely, when employing a four-edge dresser, localized plastic flow causes some grain tips to flatten and become smoother, rather than fracturing away. In Figure 13, the glossy wear surfaces on the grain tips represent grain flattening due to plastic deformation. Anyway, sharper fractured grains, which are achieved by a single-edge dresser, cause more active grains on the GW surface, which reduces surface roughness on the ground surface. It has been shown that more grain flattening achieved by a four-edge dresser generally results in increased grinding forces and rougher workpiece finishes. Figure 11 shows that by reducing the dressing depth in a single edge dresser, more grain flattening will be generated on the wheel surface, which results in increasing ground workpiece surface roughness. But by increasing the dressing feed, the surface roughness will be reduced, as the material removal rate in dressing processes increased and the sharpening and fracture of more grains will be achieved. Figure 12 indicates that by increasing the material removal rate in four-edge dressers by increasing dressing depth, a finer surface finish will be generated on the workpiece surface, as the grain fracture and sharpening will occur more in comparison to grain flattening and grain plastic deformation. The improved surface finish achieved through the application of the MQL technique is likely attributable to the enhanced lubrication of abrasive grains at the interface between the workpiece and the wheel. This enhanced lubrication facilitates smoother sliding of the chips over the tool surface, ultimately leading to a superior surface finish.

Therefore, not only the dressing feed but also the depth of dressing has significant effects on dressing performance. In addition, the dressing feed and depth behave differently on the dressing performance when using single-point or multi-point diamond dressers. The experimental results show that during grinding of Inconel 738 using a single-point dresser and a very fine dressing operation by reducing the dressing depth lower than 2 μm increases surface roughness, but applying a four-point dresser and a very fine dressing operation by reducing dressing depth and feed rate lower than 20 μm and 213 mm/min, respectively, increases surface roughness.

Figure 14 displays the surface morphology of the GW and the resulting chips when subjected to various wheel dressing conditions and types of coolant lubricants, all utilizing a four-edge dresser. This figure illustrates that the lowest chip loading occurs in wet grinding, thanks to the abundant cutting fluid, ensuring adequate fluid for efficient chip removal. Furthermore, during wet grinding, the workpiece temperature remains lower compared to grinding with the MQL technique, primarily due to the higher convection heat transfer coefficient of the fluid compared to MQL oil mist. Consequently, chips with lower temperatures are less likely to adhere to the wheel. Chips produced under fluid conditions tend to be predominantly long, thin, and lamellar, indicating that the chip formation mechanism is primarily influenced by lower temperatures. In contrast, the MQL technique yields various chip types, suggesting that the chip formation mechanism involves higher temperatures than in fluid-based grinding. When grinding with finely dressed wheels, the chips tend to fuse together due to elevated grinding forces and temperatures. Additionally, coarse dressing of the wheel results in fewer instances of chip loading compared to finely dressed wheels, attributed to the greater gaps between the grains.

Figure 15 shows the surface morphology of the ground specimens under MQL and wet conditions using a four-edge dresser under very soft dressing conditions at a dressing depth of 2 μm and two dressing speeds of 50 mm/min and 600 mm/min. These conditions are the critical conditions, which have inverse effects on the surface roughness that increased by reducing the depth of dressing the ground surface roughness. Figure 15 reveals that during the MQL grinding of Inconel 738 with very low material removal through fine dressing, several characteristics are evident on the ground surface, including plastic deformation, side flow, and thermal damage, such as the strong adhesion of chips to abrasive grains, wheel loading, and redeposition. These characteristics suggest that the primary mode of material removal is low shearing, accompanied by severe rubbing due to wear flats on the abrasive grains. Additionally, the figure illustrates the prevalence of ploughing and plastic deformation as the predominant modes of material removal. Conversely, surfaces subjected to wet grinding display fewer such defects, particularly a lack of plastic deformation. This observation suggests reduced chip loading on the wheel surface and a lower temperature in the grinding zone. Ground surfaces studied at a higher material-removal dressing process (coarse dressing) by increasing dressing speed indicate better surface quality on the ground surface and lower surface defects.

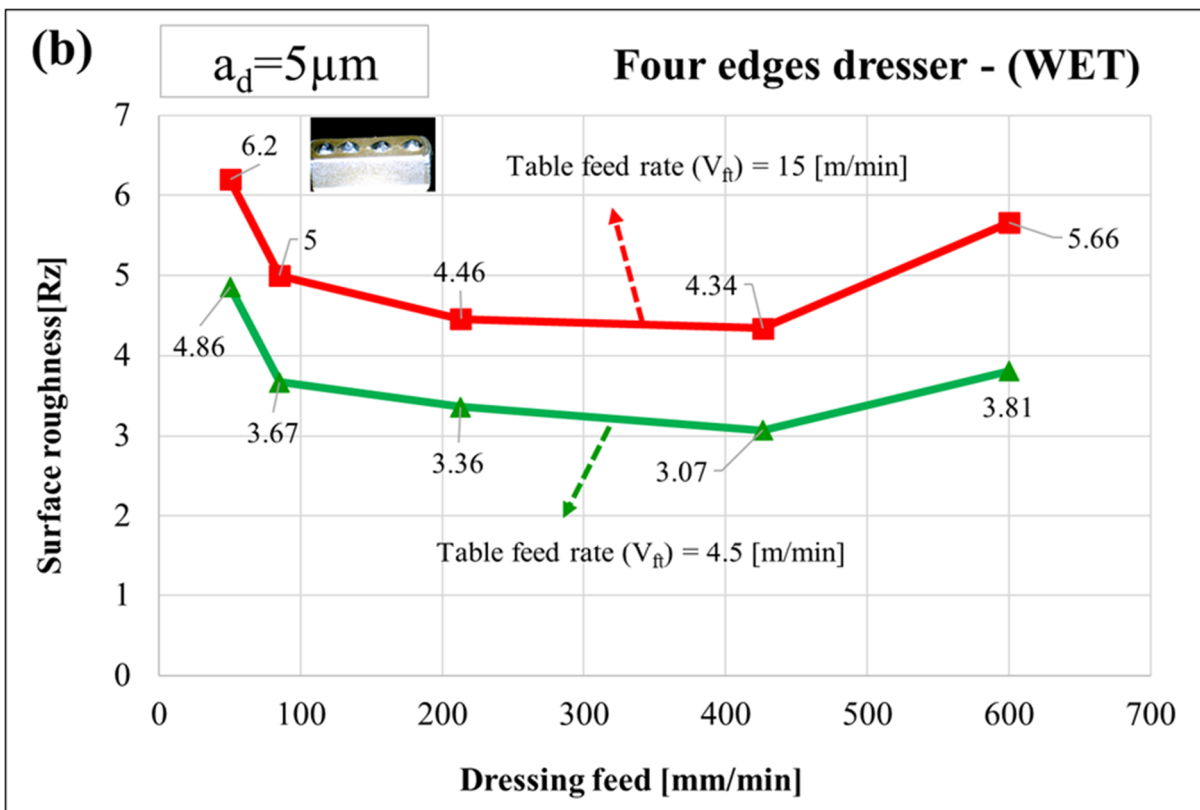
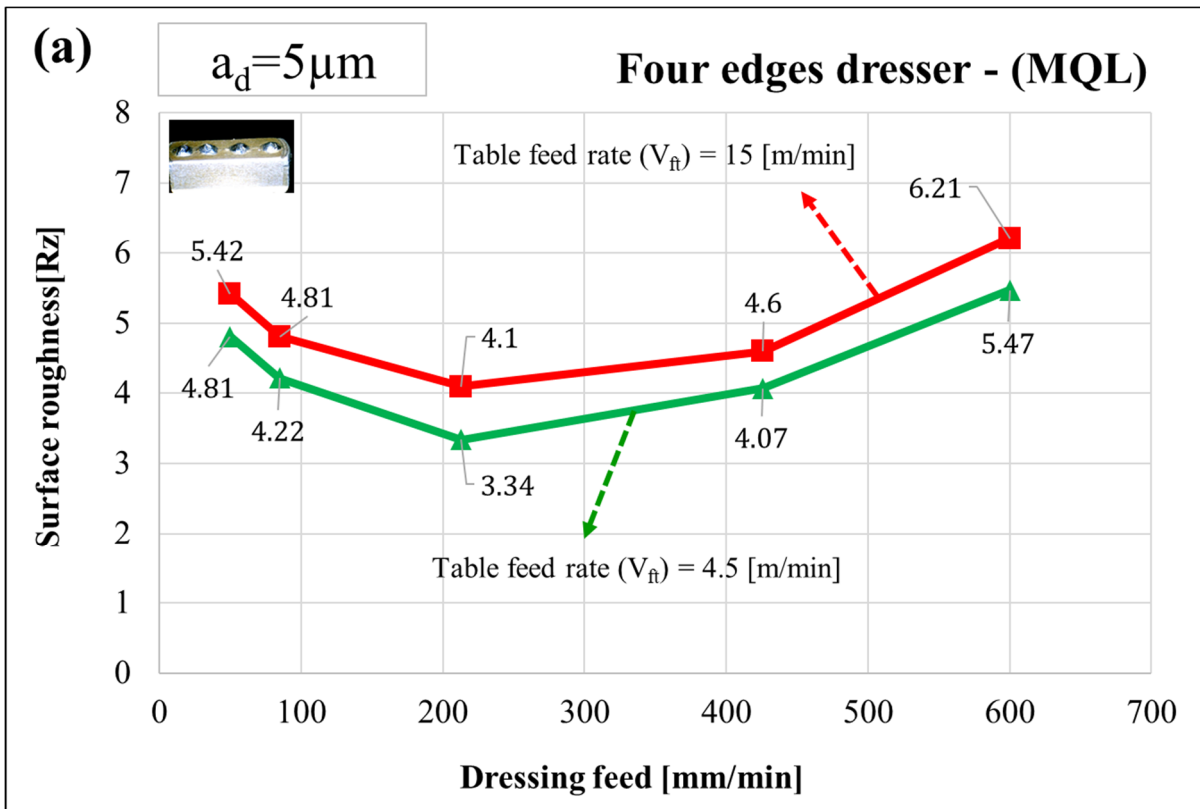


Figure 9. Workpiece surface roughness vs. dressing speed for dressing depth of $5 \mu\text{m}$ and four-edge dresser after (a) MQL grinding, (b) wet grinding.

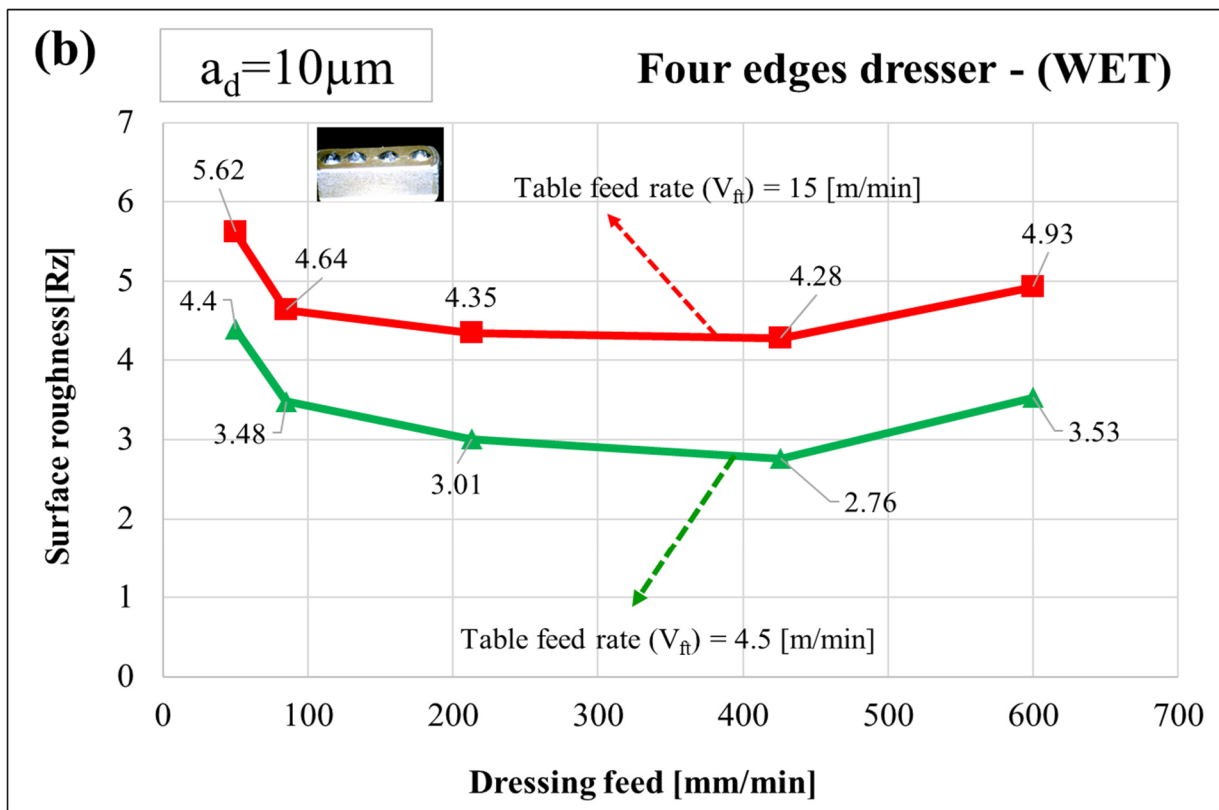
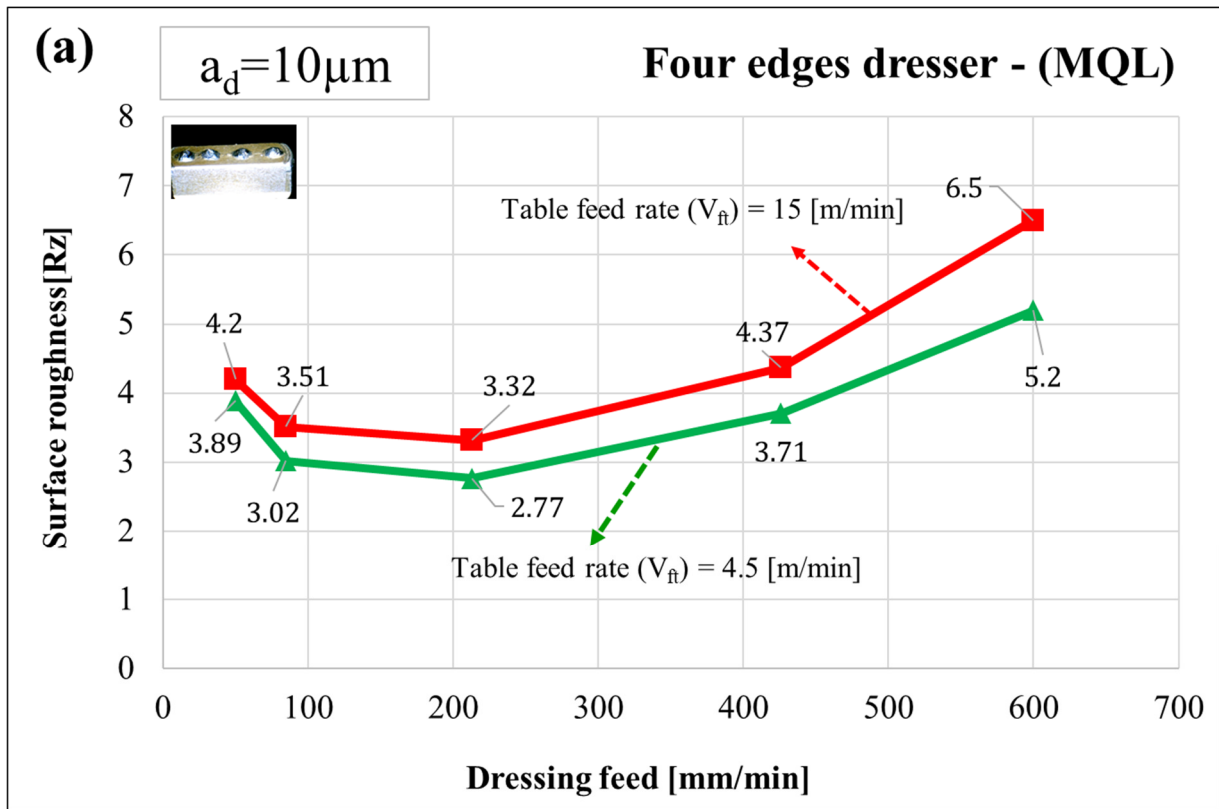


Figure 10. Workpiece surface roughness vs. dressing speed for dressing depth of 10 μm and four-edge dresser after (a) MQL grinding, (b) wet grinding.

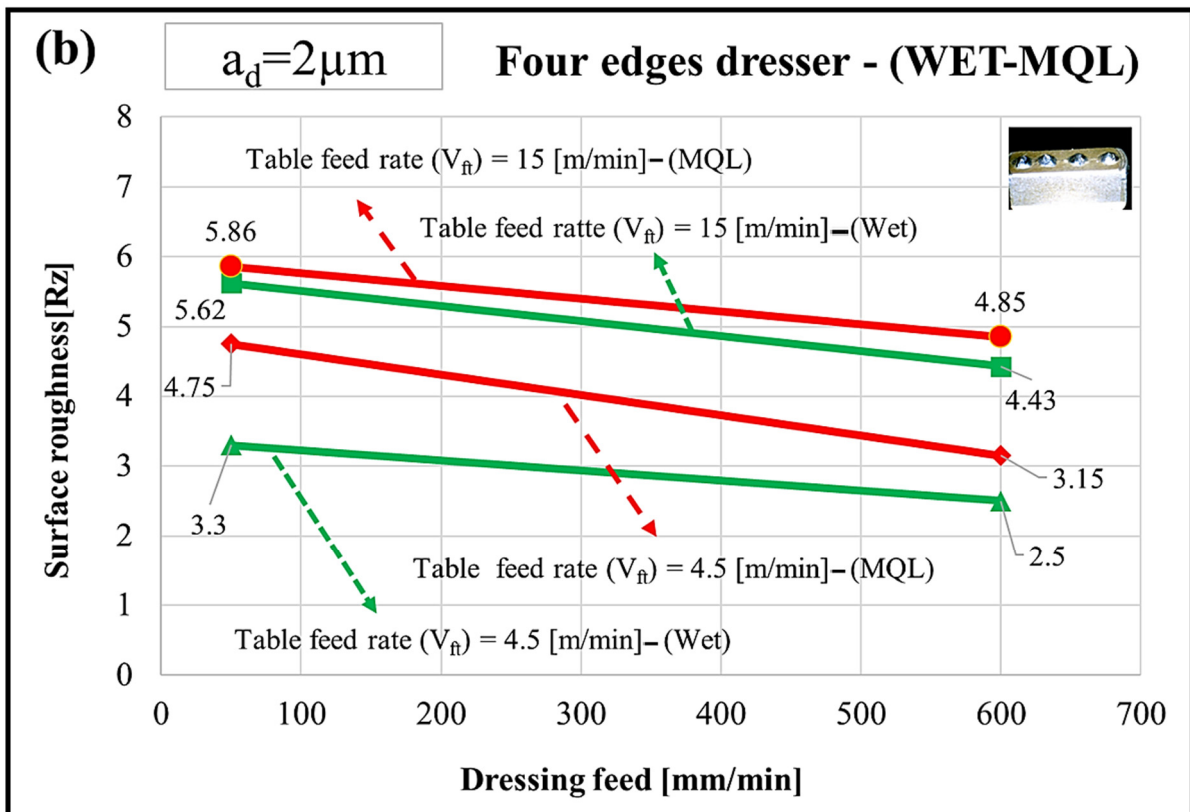
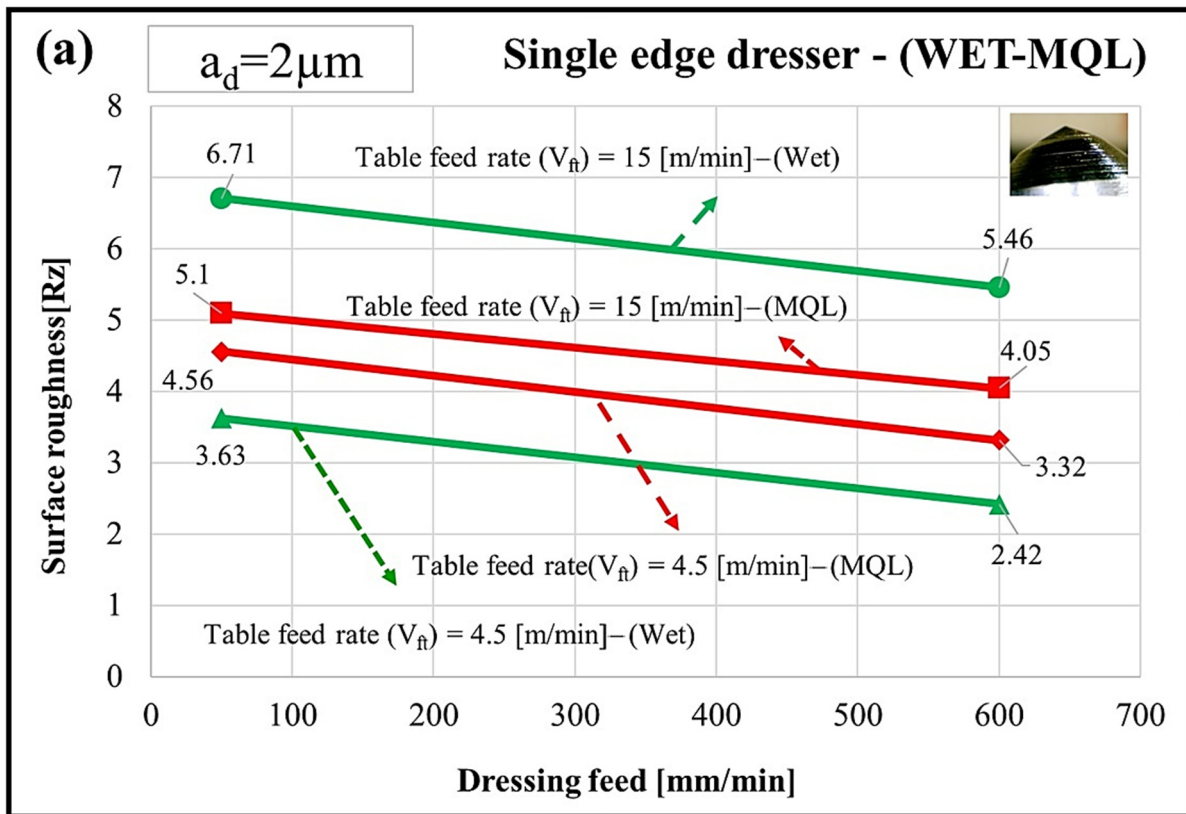


Figure 11. Workpiece surface roughness vs. dressing speed for dressing depth of $2\mu\text{m}$ and different coolant–lubricant conditions after dressing by (a) single-edge dresser, (b) four-edge dresser.

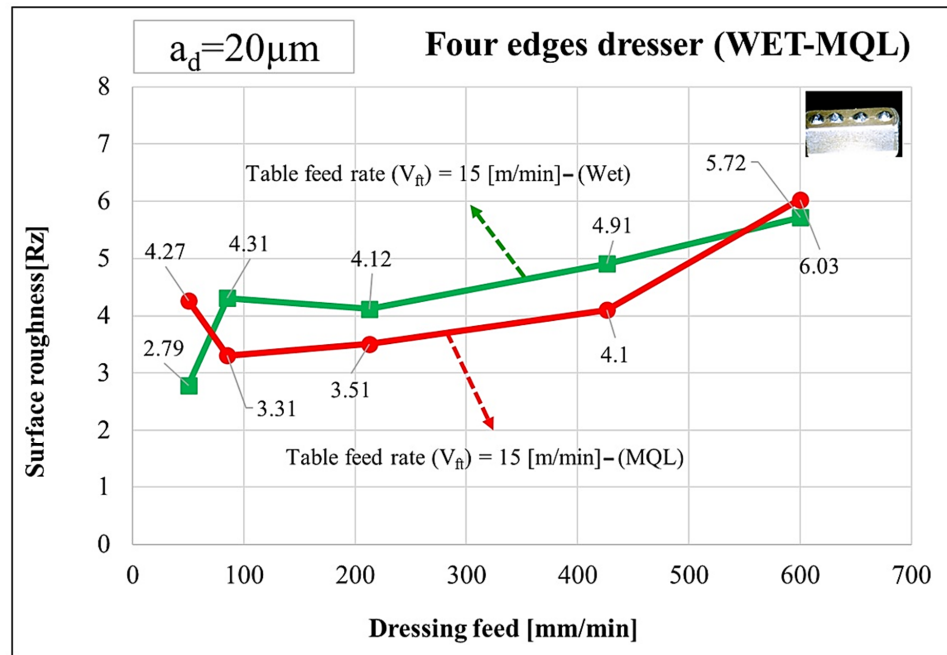


Figure 12. Workpiece surface roughness vs. dressing speed for dressing depth of 20 µm and four-edge dresser after MQL and wet grinding.

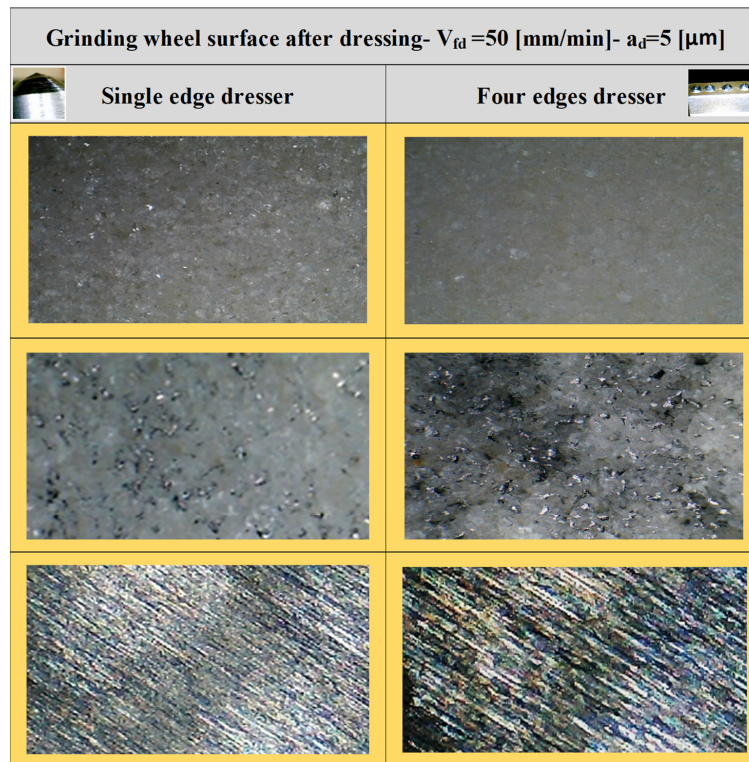


Figure 13. Detailed wheel surface topography, chip loading and workpiece surface morphology after grinding using single-edge and four-edge dressers in wet grinding of Inconel 738 with $V_{ft} = 15$ m/min, $a_e = 30$ µm and $V_c = 47$ m/s (magnification: 200×).

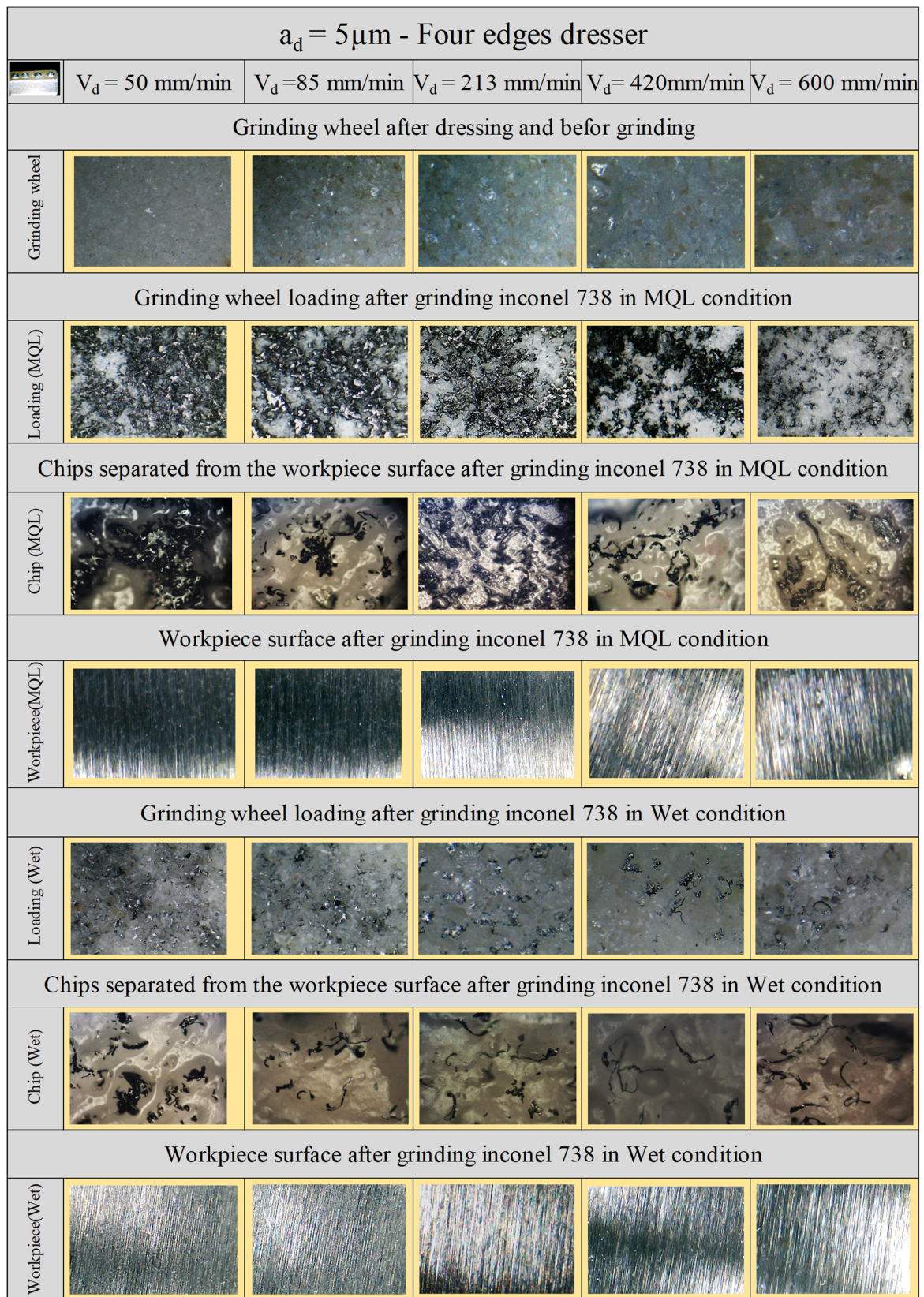


Figure 14. Cont.

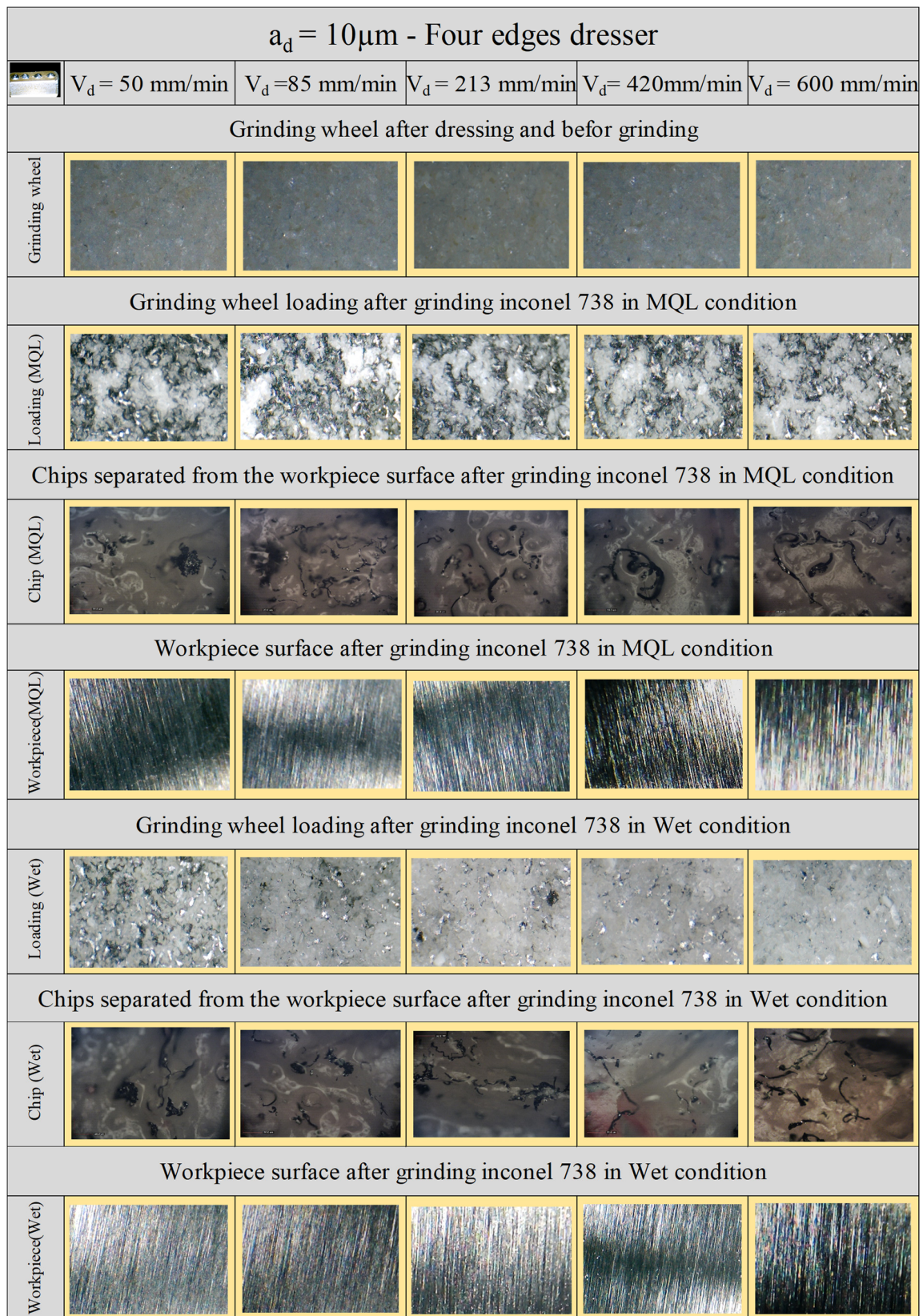


Figure 14. Surface morphology of ground workpieces, chip loading and chip morphology using four-edge dresser in MQL and wet grinding conditions ($a_e = 30\ \mu\text{m}$, $V_c = 47\ \text{m/s}$ and $V_{ft} = 4.5\ \text{m/min}$) (magnification: $200\times$).

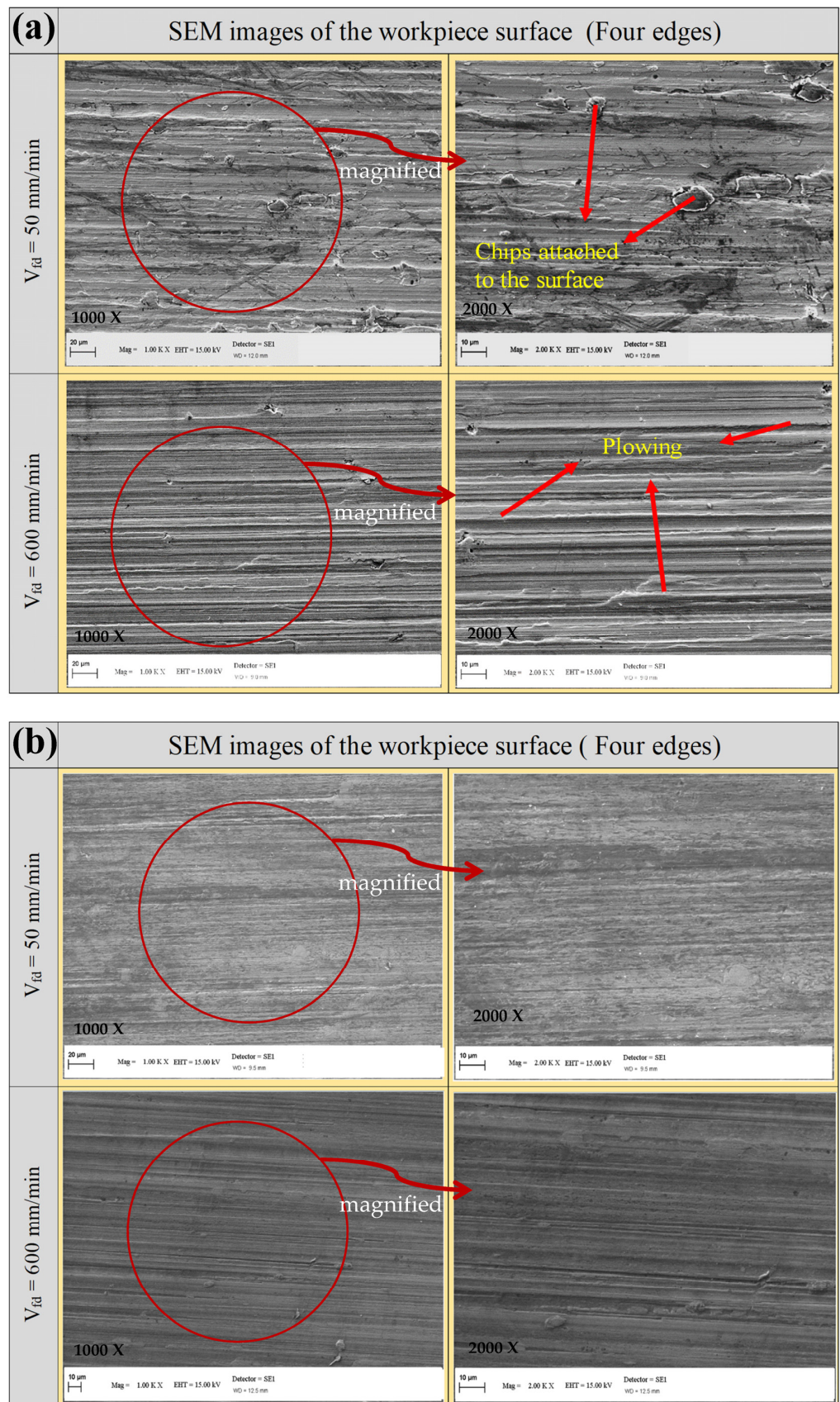


Figure 15. Surface conditions and SEM analysis of surfaces obtained when (a) MQL grinding and (b) wet grinding of Inconel 738 with four-edge dresser and $a_d = 2 \mu\text{m}$, $V_{ft} = 4.5 \text{ m/min}$, $a_e = 30 \mu\text{m}$ and $V_c = 47 \text{ m/s}$.

4. Conclusions

In the present study, for the first time, the effects of single-point and multi-point diamond dressing tools on the grinding performance of Inconel 738 have been investigated using MQL and conventional wet techniques. The most important results of this study are as follows:

1. The grinding efficiency in the MQL technique is due to the combined effects of lubrication and the appropriateness of the wheel and workpiece combinations, which are comparable to conventional wet grinding.
2. The grinding wheel surface topography has an important influence on the grinding process and it can be managed by the appropriate selection of depth of dressing and dressing speed. One of the significant results obtained in the present study is that soft dressing by decreasing the dressing material removal rate (reducing dressing depth and feed rate) will not always reduce the workpiece surface roughness. A very fine dressing process with a low material removal rate during dressing generate more grains flattening and reduce the number of active grains on the wheel surface, which increases chip loading on the wheel surface and results in more friction, sliding and plowing of grains on the workpiece surface during the grinding process.
3. Chip loading on the grinding wheel surface is one of the most critical parameters in the grinding process. Changes in dressing depth and feed rate, workpiece feed rate, and the coolant–lubricant environment can affect the amount of wheel surface loading. Due to low cutting fluid flow in the MQL technique, chip loading is significant. By rough dressing, due to the increase in depth and feed rate of the dresser, the space between the grains increases and the deposition decreases.
4. It is possible to generate surface roughness close to single-edge dressers by increasing the dressing feed rate in a four-edge dresser application while preparing the GW surface before grinding. In this case, increasing the dressing feed rate reduces dressing time and increases production capability. In addition, the lifetime of four-edge dressers is much longer than single-edge dressers.

Author Contributions: Conceptualization J.M. and M.H., Methodology: J.M. and M.H.; Software: S.A. and J.M.; Visualization: J.M. and M.H.; Validation: M.H. and J.M.; Formal analysis: J.M.; Investigation: J.M.; Resources: J.M.; Data curation: J.M., Writing—Original draft preparation: J.M. and A.M.; Writing—Review and editing: S.A.; Supervision: M.H.; Project administration: S.A. and M.H.; Funding acquisition: S.A. and M.H. All authors have read and agreed to the published version of the manuscript.

Funding: This research received no external funding.

Data Availability Statement: Data is unavailable due to privacy restrictions.

Acknowledgments: Open Access funding provided by the Qatar National Library.

Conflicts of Interest: The authors declare no conflict of interest.

Abbreviations

V_d	dressing feed rate (mm/min)
a_d	dressing depth (μm)
a_e	depth of grinding (μm)
V_{ft}	table speed (m/min)
V_s	grinding wheel speed (m/s)
S_d	dressing pitch (mm)
R_{ts}	theoretical roughness (mm)
R_z	the average maximum peak to valley of five consecutive sampling lengths within the measuring length (μm)
r_d	dresser radius (mm)
d_s	grinding wheel diameter (mm)
GW	the grinding wheel
MQL	the minimum quantity lubrication
SEM	the scanning electron microscope

References

1. Nnaji, R.N.; Bodude, M.A.; Osoba, L.O.; Fayomi, O.S.I.; Ochulor, F.E. Study on high-temperature oxidation kinetics of Haynes 282 and Inconel 718 nickel-based superalloys. *Int. J. Adv. Manuf. Technol.* **2020**, *106*, 1149–1160. [\[CrossRef\]](#)
2. Hosseini, E.; Popovich, V.A. A review of mechanical properties of additively manufactured Inconel 718. *Addit. Manuf.* **2019**, *30*, 100877. [\[CrossRef\]](#)
3. D'Addona, D.M.; Raykar, S.J. Thermal modeling of tool temperature distribution during high pressure coolant assisted turning of Inconel 718. *Materials* **2019**, *12*, 408. [\[CrossRef\]](#) [\[PubMed\]](#)
4. Qian, N.; Ding, W.; Zhu, Y. Comparative investigation on grindability of K4125 and Inconel718 nickel-based superalloys. *Int. J. Adv. Manuf. Technol.* **2018**, *97*, 1649–1661. [\[CrossRef\]](#)
5. Gu, Y.; Li, H.; Du, B.; Ding, W. Towards the understanding of creep-feed deep grinding of DD6 nickel-based single-crystal superalloy. *Int. J. Adv. Manuf. Technol.* **2019**, *100*, 445–455. [\[CrossRef\]](#)
6. Li, B.; Ding, W.; Yang, C.; Li, C. Grindability of powder metallurgy nickel-base superalloy FGH96 and sensibility analysis of machined surface roughness. *Int. J. Adv. Manuf. Technol.* **2019**, *101*, 2259–2273. [\[CrossRef\]](#)
7. Liu, Z.; Li, X.; Wang, X.; Tian, C.; Wang, L. Comparative investigation on grindability of Inconel 718 made by selective laser melting (SLM) and casting Scanning Mirror CAD Model Layers Powders Coater Laser F- θ Optic Workpiece Build Platform Powder Cartridge Feeding/Collecting System. *Int. J. Adv. Manuf. Technol.* **2019**, *100*, 3155–3166. [\[CrossRef\]](#)
8. Esmaeili, H.; Adibi, H.; Rezaei, S.M. Study on surface integrity and material removal mechanism in eco-friendly grinding of Inconel 718 using numerical and experimental investigations. *Int. J. Adv. Manuf. Technol.* **2021**, *112*, 1797–1818. [\[CrossRef\]](#)
9. De Moraes, D.L.; Garcia, M.V.; Lopes, J.C.; Ribeiro, F.S.F.; de Angelo Sanchez, L.E.; Foschini, C.R.; de Mello, H.J.; Aguiar, P.R.; Bianchi, E.C. Performance of SAE 52100 steel grinding using MQL technique with pure and diluted oil. *Int. J. Adv. Manuf. Technol.* **2019**, *105*, 4211–4223. [\[CrossRef\]](#)
10. Wojtewicz, M.; Nadolny, K.; Kapłonek, W.; Rokosz, K.; Matýsek, D.; Ungureanu, M. Experimental studies using minimum quantity cooling (MQC) with molybdenum disulfide and graphite-based microfluids in grinding of Inconel[®] alloy 718. *Int. J. Adv. Manuf. Technol.* **2019**, *101*, 637–661. [\[CrossRef\]](#)
11. Ribeiro, F.S.F.; Lopes, J.C.; Garcia, M.V.; Sanchez, L.E.d.A.; de Mello, H.J.; de Aguiar, P.R.; Bianchi, E.C. Grinding performance by applying MQL technique: An approach of the wheel cleaning jet compared with wheel cleaning Teflon and Alumina block. *Int. J. Adv. Manuf. Technol.* **2020**, *107*, 4415–4426. [\[CrossRef\]](#)
12. Ribeiro, F.S.F.; Lopes, J.C.; Garcia, M.V.; de Moraes, D.L.; da Silva, A.E.; Sanchez, L.E.d.A.; de Aguiar, P.R.; Bianchi, E.C. New knowledge about grinding using MQL simultaneous to cooled air and MQL combined to wheel cleaning jet technique. *Int. J. Adv. Manuf. Technol.* **2020**, *109*, 905–917. [\[CrossRef\]](#)
13. Malkin, S.; Guo, C. *Grinding Technology: Theory and Application of Machining with Abrasives*; Industrial Press Inc.: Norwalk, CT, USA, 2008.
14. Pande, S.J.; Lal, G.K. Effect of dressing on GW performance. *Int. J. Mach. Tool Des. Res.* **1979**, *19*, 171–179. [\[CrossRef\]](#)
15. Li, W.; Wang, Y.; Fan, S.; Xu, J. Wear of diamond GWs and material removal rate of silicon nitrides under different machining conditions. *Mater. Lett.* **2007**, *61*, 54–58. [\[CrossRef\]](#)
16. Linke, B.; Klocke, F. Temperatures and wear mechanisms in dressing of vitrified bonded GWs. *Int. J. Mach. Tools Manuf.* **2010**, *50*, 552–558. [\[CrossRef\]](#)
17. Daneshi, A.; Jandaghi, N.; Tawakoli, T. Effect of dressing on internal cylindrical grinding. *Procedia CIRP* **2014**, *14*, 37–41. [\[CrossRef\]](#)
18. Klocke, F.; Linke, B. Mechanisms in the generation of GW topography by dressing. *Prod. Eng.* **2008**, *2*, 157–163. [\[CrossRef\]](#)
19. Deng, H.; Xu, Z. Dressing methods of superabrasive GWs: A review. *J. Manuf. Process.* **2019**, *45*, 46–69. [\[CrossRef\]](#)
20. Hadad, M.; Sharbati, A. Analysis of the effects of dressing and wheel topography on grinding process under different coolant-lubricant conditions. *Int. J. Adv. Manuf. Technol.* **2017**, *90*, 3727–3738. [\[CrossRef\]](#)
21. Moreno, M.G.; Ruiz, J.Á.; Azpeitia, D.B.; González, J.I.M.; Fernández, L.G. Friction improvement via GW texturing by dressing. *Int. J. Adv. Manuf. Technol.* **2020**, *107*, 4939–4954. [\[CrossRef\]](#)
22. Zhou, L.; Wei, Q.; Zheng, N.; Chen, X.; Zhang, Q.; Wang, J. Dressing technology of arc diamond wheel by roll abrading in aspheric parallel grinding. *Int. J. Adv. Manuf. Technol.* **2019**, *105*, 2699–2706. [\[CrossRef\]](#)
23. Hacksteiner, M.; Peherstorfer, H.; Bleicher, F. Energy efficiency of state-of-the-art grinding processes. *Procedia Manuf.* **2018**, *21*, 717–724. [\[CrossRef\]](#)
24. Baheti, U.; Guo, C.; Malkin, S. Environmentally conscious cooling and lubrication for grinding. In Proceedings of the 1998 International Seminar on Improving Machine Tool Performance, San Sebastian, Spain, 6–8 July 1998; Volume 2, pp. 643–654.
25. Tönshoff, H.K.; Wobker, H.-G.; Brunner, G. CBN grinding with small wheels. *CIRP Ann.* **1995**, *44*, 311–316. [\[CrossRef\]](#)
26. Brockhoff, T.; Walter, A. Fluid minimization in cutting and grinding. *Abras. J. Abras. Eng. Soc.* **1998**, *10*, 38–42. [\[CrossRef\]](#)
27. Klocke, F.; Brinksmeier, E.; Evans, C.; Howes, T.; Lnasaki, I.; Minke, E.; Tönshoff, H.K.; Webster, J.A.; Stuff, D. High-speed grinding-fundamentals and state of the art in Europe, Japan, and the USA. *CIRP Ann.* **1997**, *46*, 715–724. [\[CrossRef\]](#)
28. Hafenbraedl, D.; Malkin, S. Environmentally-conscious minimum quantity lubrication (MQL) for internal cylindrical grinding. *Trans. Am. Manuf. Res. Inst. SME* **2000**, *28*, 149–154.
29. Silva, L.R.; Bianchi, E.C.; Catai, R.E.; Füsse, R.Y.; França, T.V.; Aguiar, P.R. Study on the behavior of the minimum quantity lubricant-MQL technique under different lubricating and cooling conditions when grinding ABNT 4340 steel. *J. Braz. Soc. Mech. Sci. Eng.* **2005**, *27*, 192–199. [\[CrossRef\]](#)

30. Lee, P.-H.; Nam, T.S.; Li, C.; Lee, S.W. Environmentally-friendly nano-fluid minimum quantity lubrication (MQL) meso-scale grinding process using nano-diamond particles. In Proceedings of the 2010 International Conference on Manufacturing Automation, Hong Kong, China, 13–15 December 2010; pp. 44–49. [[CrossRef](#)]
31. Hadad, M.J.; Tawakoli, T.; Sadeghi, M.H.; Sadeghi, B. Temperature and energy partition in minimum quantity lubrication-MQL grinding process. *Int. J. Mach. Tools Manuf.* **2012**, *54–55*, 10–17. [[CrossRef](#)]
32. Mao, C.; Huang, Y.; Zhou, X.; Gan, H.; Zhang, J.; Zhou, Z. The tribological properties of nanofluid used in minimum quantity lubrication grinding. *Int. J. Adv. Manuf. Technol.* **2014**, *71*, 1221–1228. [[CrossRef](#)]
33. Rabiei, F.; Rahimi, A.R.; Hadad, M.J.; Ashrafijou, M. Performance improvement of minimum quantity lubrication (MQL) technique in surface grinding by modeling and optimization. *J. Clean. Prod.* **2015**, *86*, 447–460. [[CrossRef](#)]
34. Setti, D.; Sinha, M.K.; Ghosh, S.; Rao, P.V. Performance evaluation of Ti-6Al-4V grinding using chip formation and coefficient of friction under the influence of nanofluids. *Int. J. Mach. Tools Manuf.* **2015**, *88*, 237–248. [[CrossRef](#)]
35. Hadad, M.; Beigi, M. A novel approach to improve environmentally friendly machining processes using ultrasonic nozzle–minimum quantity lubrication system. *Int. J. Adv. Manuf. Technol.* **2021**, *114*, 741–756. [[CrossRef](#)]
36. *DIN EN ISO 3274:1998*; Geometrical Product Specifications (GPS)—Surface Texture: Profile Method—Nominal Characteristics of Contact (Stylus) Instruments. ISO: Geneve, Switzerland, 1998.

Disclaimer/Publisher’s Note: The statements, opinions and data contained in all publications are solely those of the individual author(s) and contributor(s) and not of MDPI and/or the editor(s). MDPI and/or the editor(s) disclaim responsibility for any injury to people or property resulting from any ideas, methods, instructions or products referred to in the content.